

## Influence of the Supporting Electrolyte on the Electrochemical Polymerization of 3,4-Ethylenedioxythiophene. Effect on *p*- and *n*-Doping/Undoping, Conductivity and Morphology

M. A. del Valle<sup>1,\*</sup>, A. M. Ramírez<sup>1</sup>, L. A. Hernández<sup>1</sup>, F. Armijo<sup>1</sup>, F. R. Díaz<sup>1</sup>, G. C. Arteaga<sup>2</sup>

<sup>1</sup> Pontificia Universidad Católica de Chile, Facultad de Química, Departamento de Química Inorgánica, Laboratorio de Electroquímica de Polímeros (LEP), Vicuña Mackenna 4860, 7820436, Macul, Santiago, Chile.

<sup>2</sup> Universidad del Sinú Elías Bechara Zainum, Facultad de Ingeniería, Grupo DEMA, cra 1w N° 38-153, Montería, Colombia.

\*E-mail: [mdvalle@uc.cl](mailto:mdvalle@uc.cl)

Received: 11 May 2016 / Accepted: 17 June 2016 / Published: 7 July 2016

---

A systematic study of the influence of the type of electrochemical perturbation, in the presence of various salts, namely LiClO<sub>4</sub>, TBAClO<sub>4</sub>, TBAPF<sub>6</sub>, TEAPF<sub>6</sub>, LITFMS or TBATFMS in acetonitrile, on the electropolymerization of 3,4-ethylenedioxythiophene on platinum was accomplished. Poly(3,4-ethylenedioxythiophene) (PEDOT) electrodeposits were electrochemically characterized *in situ* while prepared by cyclic voltammetry and constant potential techniques from solutions containing the monomer and each of the abovementioned electrolytes. *n*- and *p*-doping/undoping processes (reversibility, stability and charge) and nucleation and growth mechanisms, that subsequently will be complemented and compared using conductivity measurements (four point probe method) and morphological characterization by SEM and AFM, were studied. It was verified that the volume of the supporting electrolyte ions and the waveform applied for the electrosynthesis, correlate directly with conductivity, morphology and reversibility, charge and stability of the generated polymeric coatings. Considering its likely application for the development of batteries, assessing by potentiodynamic method during 1000 cycles of charge/discharge in 0.10 mol L<sup>-1</sup> LiCl aqueous solution, it was finally corroborated that films obtained from 5 voltammetric cycles in the presence of TBAPF<sub>6</sub> are the most suitable candidates by showing, besides of reversibility, the greatest charge, with a stability larger than 95%. In any case, the results of this study allow selecting the electrosynthesis working conditions depending on the wanted application of the PEDOT modified electrode.

---

**Keywords:** 3,4-ethylenedioxythiophene, electropolymerization, *p*-doping, *n*-doping, poly(3,4-ethylenedioxythiophene), nucleation and growth mechanism.

## 1. INTRODUCTION

Conducting polymers (CP) have been extensively studied in recent years due to, inter alia, their electronic properties, suggesting them as new materials exhibiting not only stability under ambient conditions [1-3], but also useful in many and varied applications [4-6]. Among these, polythiophenes (PTH) and their derivatives such as poly(3,4-ethylenedioxythiophene) (PEDOT), show interesting properties due to its high conductivity, low band gap, low oxidation potential, high electrochemical stability [7 -15], etc. Therefore, PEDOT has become one of the most promising conducting polymers, with applications in devices as diverse as biosensors, capacitors, displays, rechargeable batteries, photodiodes, photovoltaic cells, etc. [6, 16-19].

Among the important developments in recent years, CP-based rechargeable batteries have been steadily increasing, due to the great importance that energy storage from renewable sources possesses. This has been studied by Liu *et al.* [20] that reported the fabrication of a rechargeable battery based solely on polymeric compounds. The operation of this kind of device is similar to that of lithium-ion batteries, but taken advantage of the doping/undoping process [21], incorporation-expulsion of ions, found in polymers such as Pth [22, 23], PEDOT [20, 24, 25] or polypyrrole [20, 26].

On the other hand, one of the most important problems in obtaining such material is related to its adhesion, conductivity and stability [27], which is directly related to the CP preparation procedure. To this respect, no general optimal parameters have so far been established, applicable to monomers of different nature, so that we have been searching for the best electro-synthesis conditions for each species [15]. This makes imperative to study specifically each system to optimize electropolymerization conditions according to the use envisaged for the CP electro-deposited on the working electrode.

Consequently, although there are many studies focused on the physical and chemical CPs behavior, very few studies exist that enable to relate and predict the macroscopic properties of the obtained deposit as a function of the electrosynthesis conditions. Some significant efforts have been made in this area, focused on relating the nucleation and growth mechanisms (NGM) of various CPs obtained under different experimental conditions, with their morphology and, from there, with other properties, showing that a correlation between these properties and NGM exists [28-35]. In this case, the systematic study of the effect of different salts commonly used as supporting electrolyte on the NGM, focusing mainly on correlating the type and size of the anion and cation, respectively, with the NGM and morphology of reported electrodeposited PEDOT, which are prepared varying, besides the salts, the parameters of the electrochemical system perturbation (number of potentiodynamic cycles, time of potential application, etc.), to finally find out how they affect the respective *n*- and *p*-doping/undoping processes.

## 2. EXPERIMENTAL

The monomer 3,4-ethylenedioxythiophene (EDOT) and used supporting electrolytes, namely lithium perchlorate ( $\text{LiClO}_4$ ), tetrabutylammonium perchlorate ( $\text{TBAClO}_4$ ), tetrabutylammonium hexafluorophosphate ( $\text{TBAPF}_6$ ), tetraethylammonium hexafluorophosphate ( $\text{TEAPF}_6$ ), lithium

trifluoromethylsulfonate (LITFMS) and tetrabutylammonium trifluoromethylsulfonate (TBATFMS), 99.9% were purchased from Sigma-Aldrich, while the solvent acetonitrile, CH<sub>3</sub>CN 99.9%, was Merck. The aqueous solution is prepared with lithium chloride (LiCl), Riedel de-Haen 99.9% in ultra-pure milli-Q water.

The electropolymerization was carried out in an anchor-type, three-compartment glass cell. A polycrystalline platinum (Pt) disk with a geometric area of 0.07 cm<sup>2</sup>, polished to a mirror finish with 0.3 μm alumina polishing suspension on a felt cloth, was the working electrode. A Pt wire coil of area 20-fold larger was the auxiliary electrode while the reference electrode was an Ag|AgCl electrode immersed into a tetramethylammonium chloride solution, whose concentration is adjusted so the potential matches that of a saturated calomel electrode (SCE) at room temperature [36]. All potentials quoted in the current paper are referred to this electrode.

Films growth was performed using cyclic voltammetry between -1.000 V and the most suitable anodic switching potential according to the employed salt (detailed and discussed in the next section), at a potential scan rate,  $\nu$ , 0.100 V s<sup>-1</sup>, or then at a constant potential (CP), applying a potential within a 1.180–1.360 V range (the potentiostatic disturbance was mainly applied for NGM determination). The electrolytic solution consists of 0.01 mol L<sup>-1</sup> EDOT and 0.10 mol L<sup>-1</sup> X in acetonitrile, where X = LiClO<sub>4</sub>, TBAClO<sub>4</sub>, TBAPF<sub>6</sub>, TEAPF<sub>6</sub>, LITFMS or TBATFMS.

Deposited film stability and *n*- and *p*-doping/undoping processes were assessed by studying the voltammetric response of the respective deposit in 0.1 mol L<sup>-1</sup> LiCl aqueous solutions within the corresponding potential range.

All electrochemical studies were conducted on a CH Instruments 900B potentiostat/galvanostat, at 20 °C and under a high-purity argon atmosphere.

Finally, conductivity measurements were carried out on a four-point probing Multi Hight Probe (Jandel) conductimeter and the morphology of the polymer film modified electrode was observed on a NEW Jeol IT300 SEM and picolé™ scanning probe microscope by Molecular Imaging with an AFM and STM microscope.

### 3. RESULTS AND DISCUSSION

Five successive voltammetric cycles (VC) were used to coat the Pt surface with PEDOT under potential range and rate conditions to be described in experimental. However, it must be pointed out that the potential window described in the literature when TBAPF<sub>6</sub> was used [37] must be modified when other salts are utilized, by increasing or decreasing the anodic switching potential, according to the salt used as supporting electrolyte. As seen in Table 1, the switching potential varied between 1.400 and 1.550 V ( $\Delta V$  0.150 V), the initial potential being always -1.000 V.

It is worth noting that this optimum potential was chosen considering that at lower potential virtually no deposition occurs or the film thickness increases very slowly, while at a higher potential, the behavior becomes erratic, as a result of over-oxidation of the generated polymeric film. Consequently, in each case the highest positive potential at which the recorded *i*-E profile shows a

steady current increase as a function of the successive voltammetric cycles was selected, which in this case indicates a suitable polymer film growth over the working electrode.

**Table 1.** Experimental conditions for EDOT electropolymerization upon Pt using 5 VC.

Sample	Supporting electrolyte	Potential range (V vs. SCE)	Sample	Supporting electrolyte	Potential range (V vs. SCE)
S-1	LiClO <sub>4</sub>	-1.000 – 1.500	S-6	TEAPF <sub>6</sub>	-1.000 – 1.500
S-2	LiClO <sub>4</sub>	-1.000 – 1.400	S-7	LiTFMS	-1.000 – 1.500
S-3	TBAClO <sub>4</sub>	-1.000 – 1.500	S-8	LiTFMS	-1.000 – 1.550
S-4	TBAClO <sub>4</sub>	-1.000 – 1.450	S-9	TBATFMS	-1.000 – 1.500
S-5	TBAPF <sub>6</sub>	-1.000 – 1.500	S-10	TBATFMS	-1.000 – 1.600

Voltammetric profiles recorded during EDOT electropolymerization in the presence of TBAClO<sub>4</sub> in two potential windows, corresponding to the respective ranges indicated in Table 1, are shown in Fig. 1.

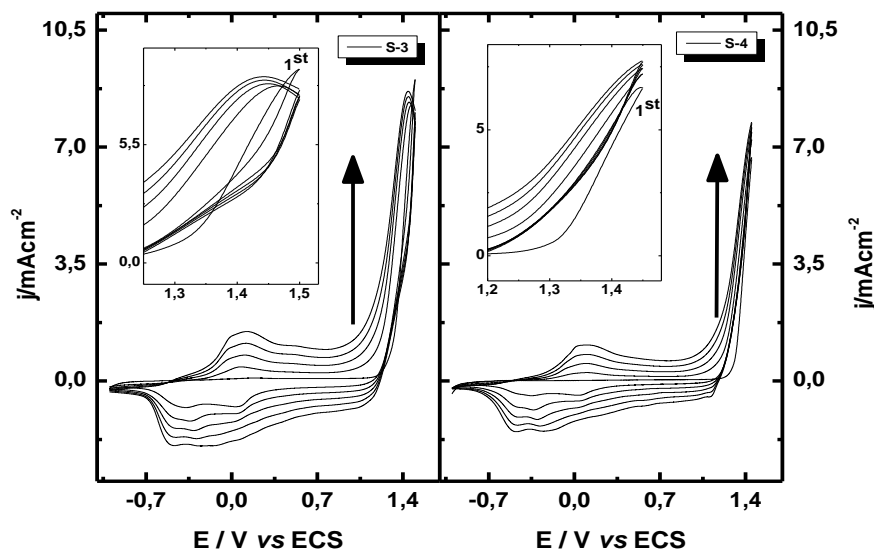


**Figure 1.** Cyclic voltammograms recorded during 5 cycles of EDOT electropolymerization on Pt at  $\square$   $0.100 \text{ V s}^{-1}$  from a  $1 \cdot 10^{-2} \text{ mol L}^{-1}$  EDOT +  $1 \cdot 10^{-1} \text{ mol L}^{-1}$  TBAClO<sub>4</sub> solution, in CH<sub>3</sub>CN. The potential windows correspond to S-3 and S-4 of Table 1.

Variation of the optimal anodic switching potential would be explained considering the anion size of the supporting electrolyte utilized for the oxidative electropolymerization considering that TFMS is 1.5 fold bulkier than ClO<sub>4</sub><sup>-</sup> [38]. Consequently the amplitude of the optimal range

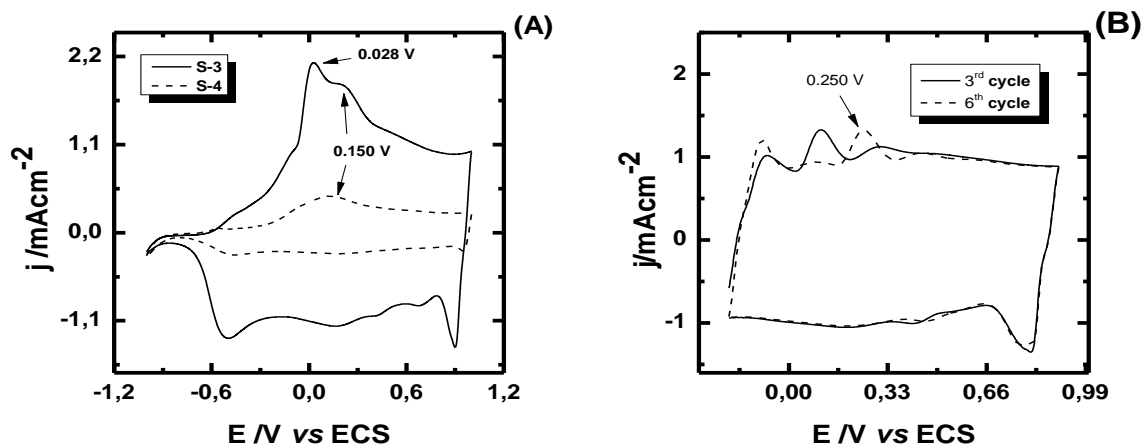
increasingly raises in the following order:  $\text{ClO}_4^- < \text{PF}_6^- < \text{TFMS}^-$ , *i.e.* directly related to the anion volume increase: a volume increase of  $14 \text{ (\AA)}^3$ , causes a potential range increase of 50 mV.

It was also verified that although the cation does not participate in the polymerization process by electro-oxidation, its size influences the potential range too since a 50 mV decrease was observed in the presence of  $\text{Li}^+$  with respect to  $\text{TEA}^+$  and  $\text{TBA}^+$ . Although the latter possess higher volumes, which varies 6.5 to 24 times, respectively, this effect could be assigned to a hindrance of the active species to diffuse towards the electrode|solution interface, generating a sort of barrier effect.

On the other hand, the voltammetric response between -1.000 and 1.000 V of the modified electrodes according to S-3 and S-4 conditions (Table 1) in the respective solution containing no monomer (Fig. 2A), show that the films obtained between -1.000 V and 1.500 V promote the appearance of a new peak at a more negative potential, 0.028 V, that overlaps film doping occurring at 0.150 V [39, 40]. Although no mention of this peak was found in the literature, it might be related to the same doping process, but corresponding to deposition of longer chains that would be generated by applying a more positive potential during the electropolymerization. These chains, in turn, being longer, would cause a twisting or winding as wool ball, behavior that is corroborated through the voltammograms corresponding to the *p*-doping/undoping process (Figs. 2B-C), since S-3 shows a not very stable response and its *p*-doping potential tends to shift to more positive values, in contrast, the films obtained at shorter potential intervals exhibit rapid stabilization and a defined *p*-doping potential.

Likewise, the respective voltammograms for the *n*-doping/undoping process (Fig. 2D), show that the films prepared at longer intervals exhibit a small shift towards less negative potentials. In addition, films synthesized at smaller potential intervals, present a capacitive current density in the 0.100 V region, where the *n*- and *p*-doping processes separation can be clearly seen.

It is worth noting that the described behavior was also observed when  $\text{LiClO}_4$  was used as supporting electrolyte, but not when  $\text{TFMS}^-$  was employed, in which case, when the electropolymerization is performed at lower anodic switching potentials, the surface coated with the polymeric film is incomplete.



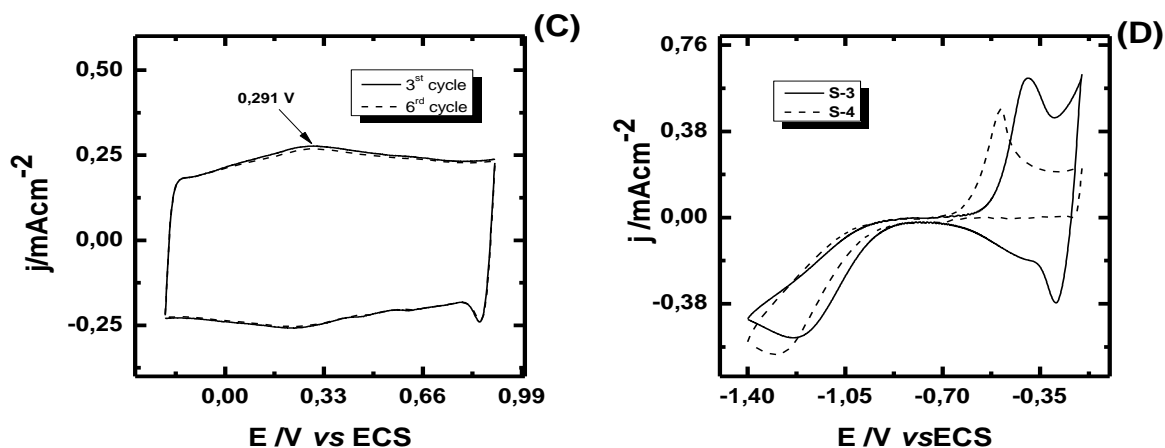


**Figure 2.** (A) Cyclic voltammograms of the Pt|PEDOT modified electrode prepared from S-3 and S-4 using  $0.10 \text{ mol L}^{-1}$  TBAClO<sub>4</sub> in acetonitrile (*p*-doping/undoping). (B) S-3 *p*-doping/undoping vs. number of voltammetric cycles. (C) S-4 *p*-doping/undoping vs. number of voltammetric cycles. (D) S-3 and S-4 *n*-doping/undoping.

*p*- and *n*-doping/undoping charge values of electrosynthesized deposits within optimal potential ranges, are summarized in Table 2. These charges were determined during the sixth voltammetric cycle of the polymer modified electrode using the same solution of the synthesis, but monomer free. A good chemical reversibility can be checked, with ratio 1, between the *p*-doping/undoping charges. Nevertheless, as often seen, the reversibility of the *n*-doping/undoping process is not optimal and even, in the case of Li<sup>+</sup>, it becomes quite irreversible. This has been ascribed to the ease that lithium ion possesses, because of its small volume ( $25.25 \text{ \AA}^3$ ), to dope, without being fully ejected when undoped, because it remains entrapped inside the polymeric matrix [38]. It is noteworthy that in each case the charge is recorded during the 6th voltammetric cycle, as to make sure that a stable response profile has been reached.

**Table 2.** *p*-( $Q_{pd}$ ,  $Q_{pu}$ ) and *n*-doping/undoping ( $Q_{nd}$ ,  $Q_{nu}$ ) charges obtained from the sixth voltammetric cycle response in electrolytic solution without monomer, within the optimal potential ranges for PEDOT electrodeposits synthesized by using five successive VC in the presence of various salts.

Sample*	$Q_{pd} / \text{mC} \cdot \mu\text{g}^{-1}$	$Q_{pu} / \text{mC} \cdot \mu\text{g}^{-1}$	$Q_{pd}/Q_{pu}$	$Q_{nd} / \text{mC} \cdot \mu\text{g}^{-1}$	$Q_{nu} / \text{mC} \cdot \mu\text{g}^{-1}$	$Q_{nd}/Q_{nu}$
S-2	0.180	0.179	1.00	0.068	0.040	1.70
S-4	0.220	0.220	1.00	0.050	0.048	1.04
S-5	1.289	1.267	1.01	0.534	0.516	1.03
S-6	0.226	0.225	1.00	0.086	0.075	1.15
S-8	0.689	0.680	1.01	0.180	0.103	1.75
S-10	0.890	0.879	1.01	0.258	0.241	1.07

\* Described in Table 1.

On the other hand, and from the cyclic voltammograms recorded during cyclic voltammetry electropolymerization, the nucleation and growth potential range was selected to study EDOT electro-oxidation at fixed potential, FP, using different supporting electrolytes in order to obtain polymeric electrodeposits respectively comparable with the above prepared products, since just the kind of electrochemical waveform has been varied.

In this case, it should be noted firstly that when the same salt is used for the electropolymerization by FP, increasing the electropolymerization potential the induction time ( $\tau$ ) decreases which corresponds to the elapsed time of the exponential decay after the initial current rise, until the rise takes place again, due to the nucleation and subsequent growth of the electrodeposit. This fact would indicate a faster nucleation over the Pt surface; this behavior has also been observed in EDOT electropolymerization in the presence of all the tested salts.

Furthermore, as for cyclic voltammetry, a variation of the optimal electropolymerization potential was verified depending on the salt used as supporting electrolyte. This variation that can be corroborated for instance in  $j/t$  transients of Fig. 3 (the cation is maintained, to analyze the effect of the anion (Fig.3a), and then the anion is fixed to study the cation effect (Fig. 3B)) and was ascribed, as when utilizing cyclic voltammetry technique, to ion volume.

Thus,  $j/t$  transients recorded during PEDOT growth at  $E_p$  1.260 V show a clear effect of ion volume on  $\tau$  and on the charge corresponding to the film growth process. However, when transients from Fig 3A are compared with those of Fig. 3B, it is possible to appreciate that the influence of anions would be more significant than that of larger cations; this was assigned to monomer diffusion towards the electrode|solution that delays the oxidation process and subsequent formation of oligomers to generate the "high density oligomeric region", HDOR, at the vicinity of the electrode surface, which is reflected in larger  $\tau$  values, while the polymerization and doping charges are lower.

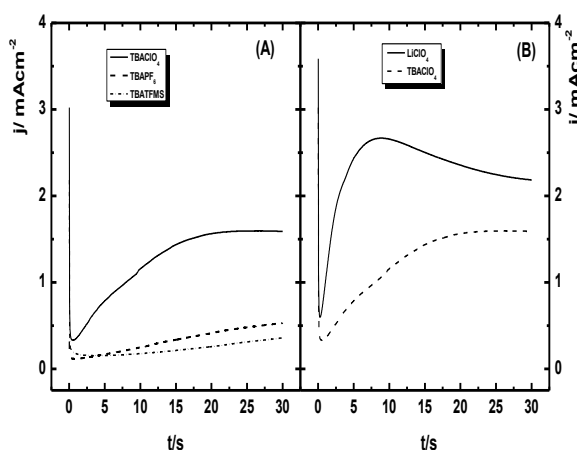


**Figure 3.**  $j/t$  transients during EDOT electropolymerization on Pt from  $0.01 \text{ mol L}^{-1}$  EDOT +  $0.10 \text{ mol L}^{-1}$  supporting electrolyte (salts in the inset),  $E = 1.260 \text{ V}$ : (A) anion size effect, and (B) cation size effect.

Table 3 summarizes the values of  $p$ - and  $n$ -doping/undoping of PEDOT films polymerized at different fixed potentials [27]. It can be observed that the electro-obtained films in the presence of

TBAPF<sub>6</sub> exhibit greater charge for both doping/undoping processes. This can be ascribed to a faster film growth, provoked by the greater basicity of PF<sub>6</sub><sup>-</sup>, as described in the literature for thiophene electropolymerization [29]. On the other hand, similarly to electropolymerization by cyclic voltammetry, the *n*-doping/undoping process in the presence of Li<sup>+</sup> exhibits less reversibility, as a result of the facility this cation would possess to go into the polymer matrix, but its low outward diffusion [38].

**Table 3.** *p*- ( $Q_{pd}$ ,  $Q_{pu}$ ) and *n*-doping/undoping ( $Q_{nd}$ ,  $Q_{nu}$ ) charges of PEDOT electrodeposits synthesized within the optimum potential ranges by FP.

Supporting electrolyte	$E_p / V$	$Q_{pd} / mC \cdot \mu g^{-1}$	$Q_{pu} / mC \cdot \mu g^{-1}$	$Q_d / Q_u$	$Q_{nd} / mC \cdot \mu g^{-1}$	$Q_{nu} / mC \cdot \mu g^{-1}$	$Q_d / Q_u$
LiClO <sub>4</sub>	1.230	0.095	0.092	1.03	0.043	0.034	1.26
TBAClO <sub>4</sub>	1.270	0.059	0.058	1.02	0.032	0.030	1.07
TBAPF <sub>6</sub>	1.340	0.176	0.173	1.02	0.049	0.050	0.98
TEAPF <sub>6</sub>	1.290	0.129	0.130	0.99	0.041	0.044	0.93
LiTFMS	1.280	0.154	0.151	1.02	0.048	0.030	1.60
TBATFMS	1.350	0.142	0.143	0.99	0.041	0.043	0.95

On the other hand, the waveform applied for EDOT electropolymerization has a clear influence on the doping/undoping charges of the polymer films, *e.g.* coatings obtained by cyclic voltammetry using the same supporting electrolyte present between 20 and 50 % more charge that when polymerized using FP.

This behavior is independent of the amount of electrosynthesized polymer and can be attributed to a more disordered growth over the electrode surface, since to maintain a fixed potential, the series of oligomerization reactions that generate an uncontrolled increase of the HDOR is triggered at the electrode vicinity. Thus, the oligomer mixture from which the precipitate that causes the polymeric deposit is formed is made of units of different chain lengths. However, using cyclic voltammetry the system receives an amount of energy that gradually varies and is used in different processes during the electropolymerization, including structure rearrangement of the produced polymer, by the undoping process, forming thus an orderly film [39, 41].

This was corroborated from conductivity measurements conducted to similar films electrosynthesized by varying just the type of applied perturbation: those generated by cyclic voltammetry showed higher conductivity than his counterpart prepared by FP, the conductivity being 50 % lower. Films electro-obtained by cyclic voltammetry in TBAPF<sub>6</sub> exhibit the highest conductivity (17.65 S cm<sup>-1</sup>), while the lowest one was recorded for films synthesized using FP in the presence of TBAClO<sub>4</sub> (7.33 S cm<sup>-1</sup>).

Therefore, conductivity can be ordered as a function of the dopant anion used for the electropolymerization. Regardless of the applied disturbance, the following decreasing sequence was found  $\text{PF}_6^- > \text{TFMS}^- > \text{ClO}_4^-$ .

To analyze the effect of these cations and anions on PEDOT NGM on Pt and to determine its likely correlation with the doping/undoping values, the respective  $j/t$  transients were deconvolved from  $\tau$ , *i.e.* by subtracting the time corresponding to the contribution by diffusion during monomer oxidation [37, 42]. Thus,  $j$  and  $t$  values are normalized according to the corresponding  $\tau$  for each electropolymerization, these coordinates are assigned by  $j(0,0)$ . Then, to determine PEDOT NGM, experimental transients obtained in the presence of different salts is deconvolved, using different equations, already well known for metal electro-deposition, which have been found are also valid for polymer films, getting errors below 2 % [16, 28-35, 37, 42]. In this case, the mechanism can be represented by Equation 1:

$$j = a[1 - \exp(-bt^2)] + ct^{-0.5}[1 - \exp(dt^2)] \quad (1)$$

Equation 1 has two contributions, where the first term corresponds to an instantaneous nucleation process with tridimensional growth (3D) controlled by charge transfer  $\text{IN}_{3\text{D}_{\text{ct}}}$ , and the second, to a *progressive nucleation* and *3D growth* mechanism under *diffusion control* ( $\text{PN}_{3\text{D}_{\text{dif}}}$ ). In this equation, the variables  $a$ ,  $b$ ,  $c$  and  $d$  correspond to:

$$a = NFk'_3 \quad (\text{Ec. 2}) \quad b = \frac{\pi M^2 k_3^2 N_{3\text{D}}}{\rho^2} \quad (\text{Ec. 3})$$

$$c = \frac{\pi FD^{1/2} C_\infty}{\rho^{1/2}} \quad (\text{Ec. 4}) \quad d = \frac{A' k \pi D}{2} \quad (\text{Ec. 5})$$

where  $F$ ,  $M$  and  $\rho$  are known and conventionally used parameters,  $N_{3\text{D}}$  is the number of nuclei formed at  $t = 0$ ,  $k_3$  and  $k'_3$  are rate constants of 3D nuclei growing parallel and perpendicular to the electrode surface,  $D$  and  $C_\infty$  are respectively the diffusion coefficient and monomer concentration in the bulk solution. Finally,  $A'$  and  $k$  are described by another mathematical algorithm represented by:

$$A' = AN_{\text{dif}} \quad (6) \quad y \quad k = \frac{3}{4} \left( \frac{8\pi C_\infty M}{\rho} \right)^{1/2} \quad (7)$$

where  $N_{\text{dif}}$  is the number of nuclei formed at  $t = 0$  that grow under diffusion control and  $A$  is the nuclei formation rate constant.

Figure 4A shows, as example, detailed deconvolution of a transient utilizing Eq. 1, with their respective independent contributions, for EDOT electropolymerization from 0.01 mol L<sup>-1</sup> EDOT solution and 0.10 mol L<sup>-1</sup> LiClO<sub>4</sub>. It is noteworthy that, initially, the NGM is largely governed by  $\text{IN}_{3\text{D}_{\text{ct}}}$  and then at  $t > 13$  s the  $\text{PN}_{3\text{D}_{\text{dif}}}$  contribution mainly prevails. It is worth noting that these contributions are consistent with those previously reported for this kind of polymer [37, 43].

Moreover, Figs. 4B-C reveal that increase of the electropolymerization potential,  $E_p$ , promotes diffusion controlled process. Thus, the  $\text{IN}_{3\text{D}_{\text{ct}}}$  contribution governs for a shorter time than  $\text{PN}_{3\text{D}_{\text{dif}}}$ . That is, if the correlation between these previously corroborated NGM and deposit morphology is

considered [28, 29, 33-35], in the electropolymerization carried out at 1.220 V, the growth of uniform or similar size cones (being an instantaneous nucleation), would prevail during the first 17 s, providing 61 % of the total charge; subsequently,  $PN3D_{dif}$  contribution takes over, now corresponding to growth as hemispheres whose size depends on time, since in this process the nucleation is progressive. If the electropolymerization is conducted between 1.230 and 1.240 V, the mechanism remains the same. Only the time every contribution prevails is observed, although its contribution does not change so significantly, which was ascribed to the growth rate due to the potential increase:  $IN3D_{ct}$  decreases to 13 and 7 s, representing respectively 60 and 59 % of the total charge.

Parallel, and at optimum electropolymerization potentials, with  $TBAClO_4$  at  $t < 7$  s,  $IN3D_{TC}$  prevails too (62 % of the total charge). While in the case of  $TEAPF_6$  and  $TBAPF_6$  salts, 61 and 59 % was respectively obtained, and  $IN3D_{ct}$  predominates.

Finally, with respect to  $LiTFMS$  and  $TBATFMS$  salts, they presented the highest  $IN3D_{TC}$  contribution, 80 and 70 %, respectively. The increase of this contribution might be ascribed to the size of the dopant anion, because the nuclei coalesce more slowly and, therefore, the roughness should be greater. This would be consistent with the fact that the HDOR density in the latter case is larger than in the presence of ions with smaller ionic radius, forming longer-chain oligomers.

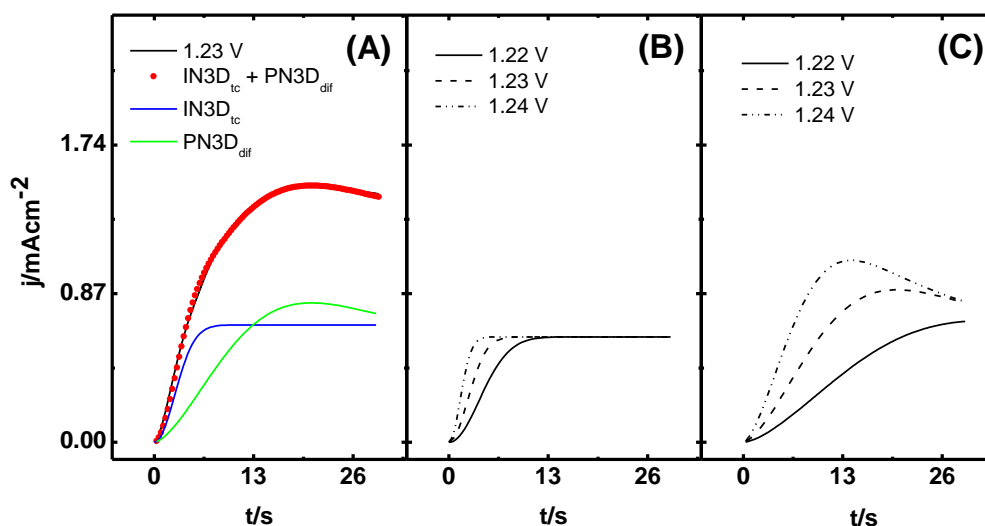


**Figure 4.** (A)  $j/t$  transient at  $E_p = 1.230$  V, between  $0 < t < 30$  s: <sup>15</sup> experimental and (●) fitted according to equation (1). Interface:  $Pt|0.01 \text{ mol}\cdot\text{L}^{-1} \text{ EDOT} + 0.10 \text{ mol}\cdot\text{L}^{-1} \text{ LiClO}_4, \text{ CH}_3\text{CN}$ . (B)  $IN3D_{ct}$  contribution vs.  $E_p$ . (C)  $PN3D_{dif}$  contribution vs.  $E_p$ .

Values of  $a$ ,  $b$ ,  $c$  and  $d$  parameters obtained from deconvolution of experimental curves in the presence of the different salts employed in this work are shown in Table 4. For  $IN3D_{ct}$  contribution it was observed that for every supporting electrolyte,  $a$  remains constant, regardless of the applied potential, while  $b$  increases in direct proportion to the potential increase. This is quite consistent, considering that  $a$  is related to nuclei perpendicular growth over the electrode surface, while  $b$  is directly related to the number of nuclei formed over the electrode surface. Accordingly and because the energy delivered to the system increases as higher potential is applied, while at the same time the number of nuclei formed on the surface takes less, explaining why the  $IN3D_{ct}$  contribution needed less

time to reach the plateau and then the process becomes diffusion-controlled, ascribed to the rapid depletion of the monomer available at the electrode|solution interface.

It is noteworthy to mention that in all cases the same order of magnitude and similar profiles are reached.

**Table 4.** Effect of experimental parameters on the numerical constants of equation (1).

EDOT / mol L <sup>-1</sup>	Supporting electrolyte salt	/ mol L <sup>-1</sup>	E / V	$\tau$ / s	a / mA cm <sup>-2</sup>	b / s <sup>-2</sup>	c / mA cm <sup>-2</sup> s <sup>-1/2</sup>	d / s <sup>-2</sup>
0.01	LiClO <sub>4</sub>	0.10	1.220	0.96	0.61731	0.03226	4.428	0.00234
			1.230	0.66	0.61731	0.08498	4.428	0.00580
			1.240	0.46	0.61731	0.23846	4.428	0.01174
0.01	TBAClO <sub>4</sub>	0.10	1.260	0.50	0.56223	0.03618	4.009	0.00329
			1.270	0.38	0.56223	0.16330	4.009	0.00869
			1.280	0.32	0.56223	0.48025	4,009	0.01417
0.01	TBAPF <sub>6</sub>	0.10	1.330	0.22	0.62070	0.10714	3.540	0.00606
			1.340	0.12	0.62070	0.42810	3.540	0.01983
			1.350	0.10	0.62070	0.63679	3.540	0.03733
0.01	TEAPF <sub>6</sub>	0.10	1.280	1.26	0.53770	0.02444	4.957	0.00243
			1.290	0.69	0.53770	0.08790	4.957	0.01366
			1.300	0.64	0.53770	0.17092	4.957	0.01441
0.01	LiTFMS	0.10	1.270	0.48	0.75271	0.03142	1.316	0.00232
			1.280	0.44	0.75271	0.08194	1.316	0.00584
			1.290	0.28	0.75271	0.17047	1.316	0.03922
0.01	TBATFMS	0.10	1.340	0.16	0.84943	0.28698	2.117	0.01058
			1.350	0.12	0.84943	0.58885	2.117	0.02450
			1.360	0.10	0.84943	0.91865	2.117	0.03922

On the other hand, for the  $PN3D_{\text{dif}}$  contribution,  $c$  does not change with the applied potential for the same electrolyte, which can be explained considering that this variable mainly contains the diffusion coefficient, which is independent of the applied potential. Conversely, for different supporting electrolytes, in Table 4 it can be found how this parameter varies for the two reasons that would confirm the hypothesis proposed herein: i) the larger size of the anion would generate a nucleation delay, increasing the time they take to coalesce to form a new growing surface over the electrode and ii) the cation also produces a hindrance, barrier effect type, for the arrival of the monomer to the electrode surface.

To corroborate these statements, from equation (4) diffusion coefficients,  $D$ , are determined, depending on the salt used, Table 5. A  $D$  decrease in the presence of cations or anions of large size was

verified and even when both ions increase their size, the diffusion coefficient goes down by one order of magnitude.

**Table 5.** Volume effect of cation and anion used in the supporting electrolyte on EDOT diffusion coefficient.

Supporting electrolyte salt	Cation volume / $\text{\AA}^3$ [38]	Anion volume / $\text{\AA}^3$ [38]	$D$ / $\text{cm}^2 \text{s}^{-1}$
$\text{LiClO}_4$	25.25	57.09	$3.597 \cdot 10^{-3}$
$\text{TBAClO}_4$	300.40	57.09	$1.172 \cdot 10^{-3}$
$\text{TEAPF}_6$	164.34	71.35	$1.450 \cdot 10^{-3}$
$\text{TBAPF}_6$	300.40	71.35	$1.037 \cdot 10^{-3}$
$\text{LiTFMS}$	25.25	85.20	$6.856 \cdot 10^{-4}$
$\text{TBATFMS}$	300.40	85.20	$3.190 \cdot 10^{-4}$

In addition, the values obtained in the presence of  $\text{TFMS}^-$ , are lower than those recorded in the presence of the other studied anions, which can be attributed to that in this case the NGM becomes mainly governed by the  $\text{IN3D}_{\text{ct}}$  contribution (almost 80 % of the total charge).

As for the parameter  $d$ , involving the number of nuclei formed on the working electrode, whose growth is controlled by the diffusion of monomer to the interface, similar profiles are observed, noting just the charge decrease after the maximum is reached, when the applied electropolymerization potential increases. However, the magnitude practically remains unchanged, because the polymer-on-polymer growth regime has yet been reached; *i.e.* only elongation of the already formed chains occurs.

Figures 5A-C show SEM micrographs of PEDOT films obtained by cyclic voltammetry, wherein a homogeneous and compact film, with small conical structures on the surface, is found for  $\text{PEDOT|ClO}_4^-$ , consistent with the kind of film growth. However, the  $\text{PEDOT|TFMS}^-$  film shows less homogeneity and is less compact, which correlates with the morphology of electrosynthesized deposits in the presence of dopant anions of smaller radius. At the same time, in  $\text{PEDOT|TFMS}^-$  films little or almost no influence of the cation was observed from the morphological point of view, confirming that the size of the cation only prevents the free diffusion of the monomer to the electrode surface, delaying its oxidation.

On the other hand, Fig. 5D shows the SEM micrograph of nuclei obtained by FP electropolymerization, which allows correlating the proposed NGM. It can be seen that the morphology corresponds mainly to a conic growth, in agreement with  $\text{IN3D}_{\text{ct}}$  contribution, plus small hemispherical nuclei of various sizes, attributable to the  $\text{PN3D}_{\text{dif}}$  contribution, as predicted by the NGM established from the deconvolved transients (Figs. 5E-F). Besides, the ratio between the amount

of conic nuclei and hemi-spheres is related to the fact that one contribution is instantaneous and the other progressive and with its percentage of contribution to the overall process.

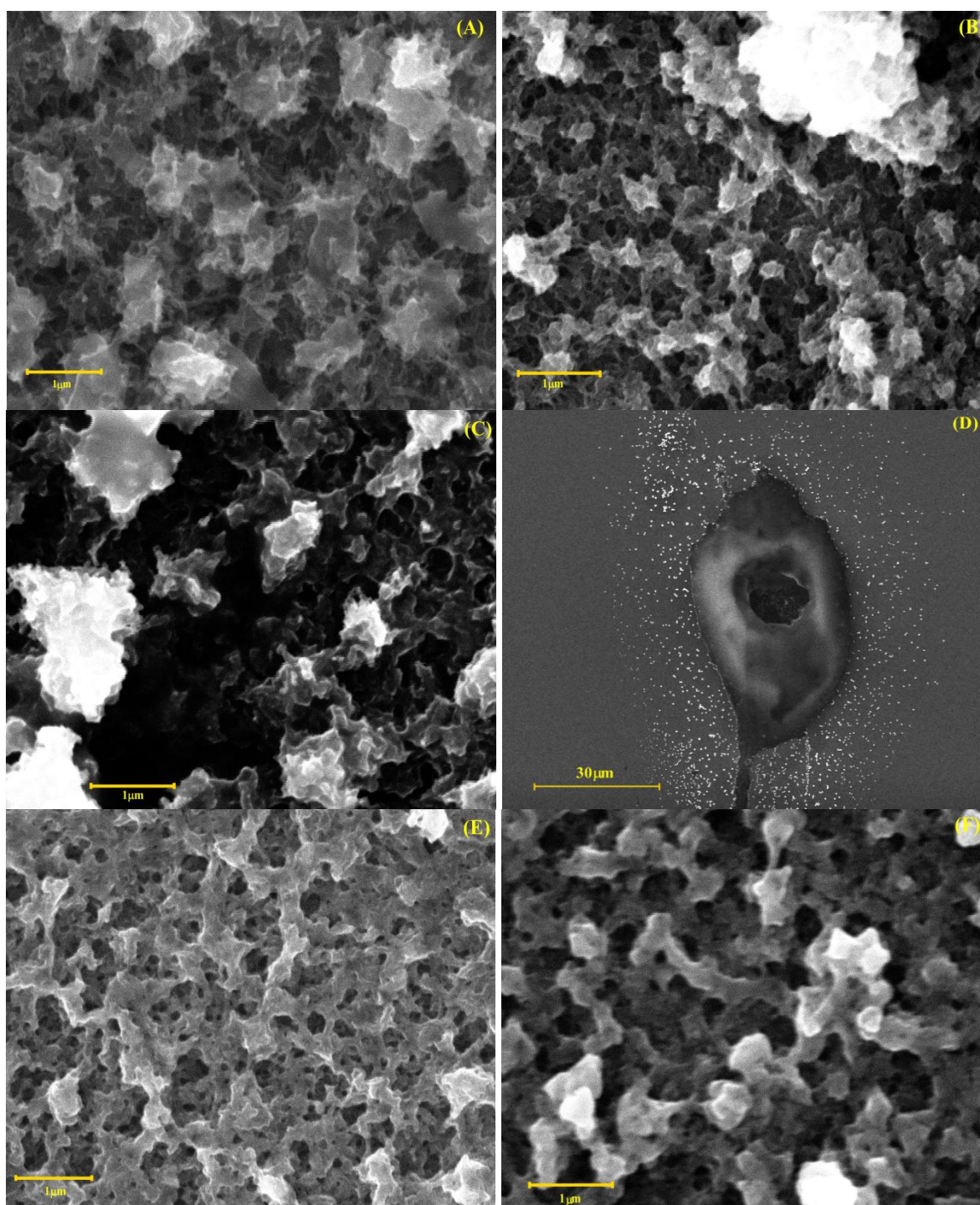


**Figure 5.** SEM micrographs of PEDOT electro-synthesized in the presence of different salts, using cyclic voltammetry: (A) TBAClO<sub>4</sub>, B) TBATFMS and (C) LiTFMS and FP: (D) TBAPF<sub>6</sub> (E) LiClO<sub>4</sub> and (F) LiTFMS. In each case, the electrodeposits were prepared employing the respective optimum conditions ( $E_p$  or potential range, according the perturbation).

This morphological analysis also enables verifying the effect of dopant anion size, since a more homogeneous morphology was observed when electro-polymerized in the presence of  $\text{LiClO}_4$  than in  $\text{LiTFMS}$ .

AFM micrographs of PEDOT films electro-synthesized from EDOT using cyclic voltammetry under the optimal potential ranges in the presence of  $\text{TEAPF}_6$  and  $\text{LiTFMS}$  respectively, are depicted in Figs. 6A-B. In both instances a compact coating on the electrode surface, with the same thickness, was obtained. In calculating the average value of the square of the roughness,  $R_q$ , of these deposits (Table 6), a slight trend to increase in the following order  $\text{ClO}_4^- < \text{PF}_6^- < \text{TFMS}^-$  was observed. Again, this small porosity variation can be explained considering the size of each dopant anion used, whose volumes are 57.09, 71.35 and 85.20  $\text{\AA}^3$ , respectively.

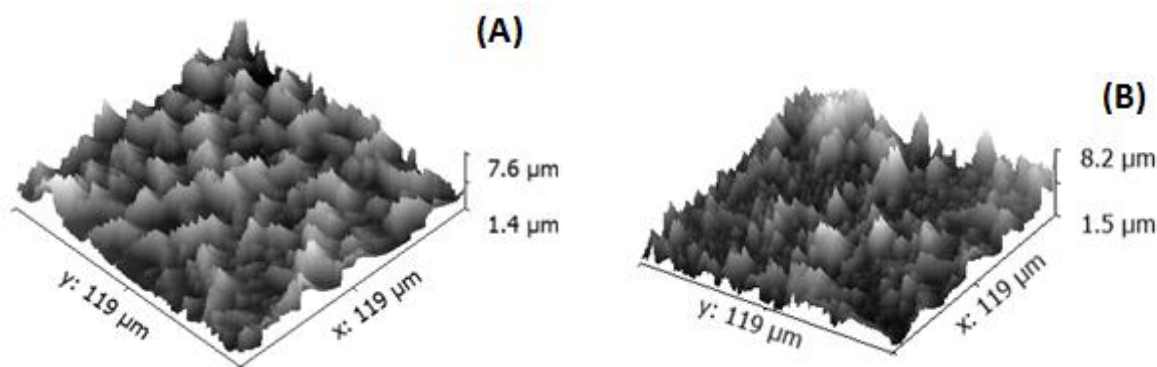


**Figure 6.** AFM micrographs of PEDOT electro-synthesized by 5 VC in the presence of (A)  $\text{TEAPF}_6$ . (B)  $\text{LiTFMS}$ .

**Table 6.** Average of the squared roughness calculated for electro-synthesized PEDOT using 5 VC in the presence of various salts.

Supporting electrolyte salt	$R_q$ ( $\mu\text{m}$ )	Supporting electrolyte salt	$R_q$ ( $\mu\text{m}$ )
$\text{LiClO}_4$	0.022	$\text{TBAPF}_6$	0.026
$\text{TBAClO}_4$	0.024	$\text{LiTFMS}$	0.030
$\text{TEAPF}_6$	0.026	$\text{TBATFMS}$	0.030

Generally speaking, the excellent correlation of the results obtained in this systematic study concerning morphology, conductivity and doping/undoping processes as a function of the electro-synthesis conditions, with respect to the electrochemical waveform applied and the supporting electrolyte employed, can be highlighted. From these results, it can now be ensure that, in the case of PEDOT, the electrodeposit of higher conductivity and better *p*-doping/undoping process (greater charge and reversibility), would be those obtained through cyclic voltammetry in the presence of  $\text{TBAPF}_6$ . Therefore, it is possible to project its use in the fabrication of rechargeable batteries.

To corroborate this possible utility, finally the study of stability and reversibility of the *p*-doping/undoping process of the films during 1000 cycles will be performed. To this end, the response of each deposit in an 0.10 mol L<sup>-1</sup> LiCl aqueous solution will be analyzed. First of all, Fig. 7 shows that the obtained films have good chemical reversibility ( $Q_{pd}/Q_{pu} = 1$ ), behavior that is repeated for all films studied under these same conditions.

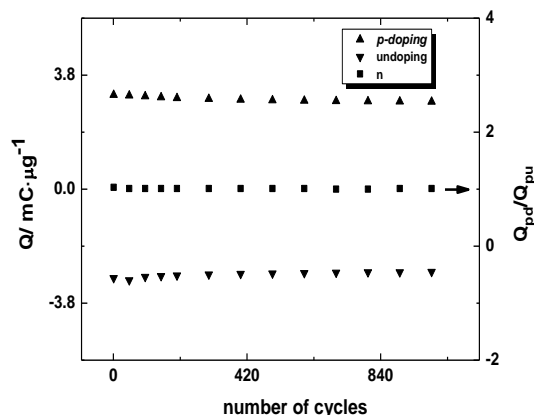


**Figure 7.** Graphical representation of the *p*-doping/undoping process in aqueous solution 0.1 mol L<sup>-1</sup> LiCl vs. number of cycles of PEDOT films electro synthesized by 5 VC in TBAPF<sub>6</sub> solution in acetonitrile as solvent.

**Table 7.** *p*- and *n*-doping/undoping charges in an aqueous solution of LiCl of PEDOT films obtained by 5 VC in the presence of various salts.

Supporting electrolyte salt	<i>p</i> -doping/undoping			<i>n</i> -doping/undoping		
	$Q_{pd}/mC \cdot \mu g^{-1}$	$Q_{pu}/mC \cdot \mu g^{-1}$	$n(Q_{pd}/Q_{pu})$	$Q_{nd}/mC \cdot \mu g^{-1}$	$Q_{nu}/mC \cdot \mu g^{-1}$	$n(Q_{nd}/Q_{nu})$
LiClO <sub>4</sub>	1.0454	0.9801	1.06	2.5092	2.3967	1.05
TBAClO <sub>4</sub>	0.7826	0.7269	1.07	1.1683	1.0842	1.09
TBAPF <sub>6</sub>	1.4161	1.3585	1.04	1.9147	1.6955	1.15
TEAPF <sub>6</sub>	1.1269	1.1160	1.02	1.2241	1.1617	1.03
LiTFMS	1.0915	1.0647	1.02	1.4789	1.3361	1.10
TBATFMS	0.6700	0.6339	1.05	0.8935	0.7618	1.18

Table 7 exhibits charge values recorded during the *p*- and *n*-doping/undoping processes of films obtained by 5 VC. It is worth noting that in this case the charges are related to the amount of electro-obtained polymer, which was calculated from the voltammograms recorded during the growth, subtracting the reduction charge to oxidation, as doping/undoping is considered reversible, then the reduction charge (equivalent only to undoping) is equal to that of doping. Therefore, if subtracted to

the oxidation charge, the polymerization charge is obtained, as the anodic charge includes both the polymerization and doping processes. It is noteworthy that in all these cases the obtained values are similar in order of magnitude to that reported by Hillman *et al.* [41] for PEDOT. As can be seen, once again it was corroborated that films prepared in the presence of TBAPF<sub>6</sub> exhibit a higher charge than that obtained with the other salts involved in this research.

Figures 8A-B shows charge stability of *p*-doping/undoping after 1000 voltammetric cycles for different films prepared by cyclic voltammetry and FP respectively. Both techniques allowed determining that films synthesized in the presence of PF<sub>6</sub><sup>-</sup> exhibit improved stability during 1000 cycles, since the charge never dropped below 93 % as compared to the initial charge. In contrast, the films prepared in the presence of ClO<sub>4</sub><sup>-</sup> exhibit much lower stability, reducing its charge to *ca.* 80-85 %. Moreover, this trend does not change for the stability of the *n*-doping/undoping process (Figs. 8C-D) because it is important to bear in mind that for both types of films (prepared by cyclic voltammetry or FP), the charge decreases below 80 % of the initial value. However, for both *p*- and *n*-doping processes, films synthesized by cyclic voltammetry are more stable, which is ascribed to its higher homogeneity and adhesion, allowing oxidation and/or partial reduction less detrimental for the film, as it has been described in the literature [15].

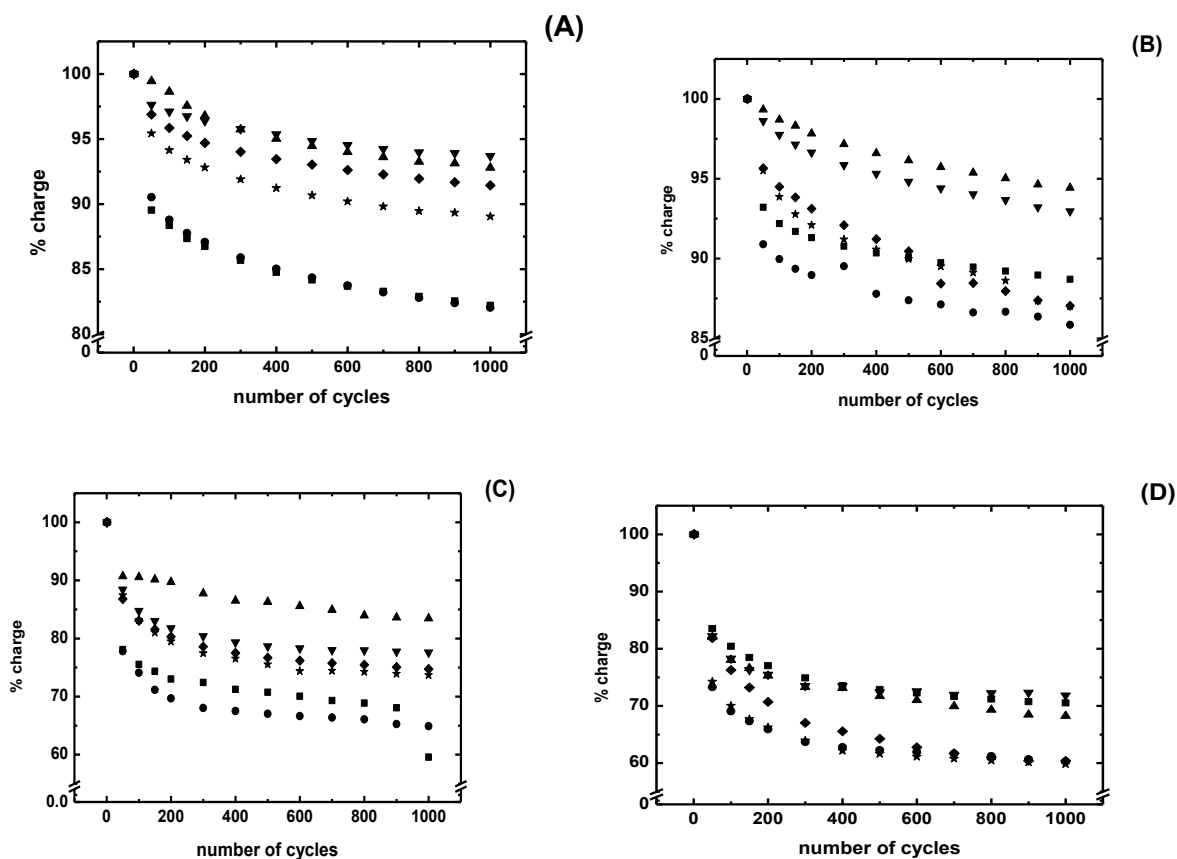


**Figure 8.** Graphical display of % charge vs. number of cycles of the doping/undoping in 0.1 mol L<sup>-1</sup> LiCl aqueous solution of polymers electrosynthesized in the presence of various salts through: (A) cyclic voltammetry and (B) FP (*p*-process). (C) cyclic voltammetry and (D) FP (*n*-process). Salts: (■) LiClO<sub>4</sub>, (●) TBAClO<sub>4</sub>, (▲) TBAPF<sub>6</sub>, (▼) TEAPF<sub>6</sub>, (◆) LiTFMS and (★) TBATFMS.

From these results, like those shown in Table 7, it is possible to verify that charge and stability of the films showed the same trend, which allows ordering in a decreasing manner the value and stability of the obtained charge depending on the type of anion used in the electropolymerization:  $\text{PF}_6^- > \text{TFMS}^- > \text{ClO}_4^-$ . In the case of  $\text{PF}_6^-$  and  $\text{TFMS}^-$  this trend can be explained by its roughness, although this is not consistent with what is presented by deposits electrosynthesized in the presence of  $\text{ClO}_4^-$ ; this finding could be explained by the difficulty of this type of salts to get dried [29], preventing good reproducibility of the electro-obtained film, as already described in the literature [44].

#### 4. CONCLUSIONS

It has been found that the doping/undoping process is closely related to the type of electrochemical perturbation (potential range, potential and electrolysis time, depending on the case) and correlates directly with the volume of ions of the salt used as supporting electrolyte, as well as conductivity and morphology of the electrodeposited polymer. Anyway, despite of varying roughness, conductivity remains within the same order of magnitude. Having in mind their possible use in battery development, films obtained with five voltammetric cycles in the presence of  $\text{TBAPF}_6$  are the most suitable candidates (exhibit high reversibility, greater charge and stability higher than 95 %). Finally, the results of this systematic study demonstrated the importance of investing time in this kind of work, because, although it is quite cumbersome to perform, helps to easily select the electrosynthesis conditions depending on the wanted utility to be given to the PEDOT modified electrode, *e.g.* if roughness or porosity will be enhanced above reversibility of the doping/undoping process or the conductivity above the homogeneity of the deposit, etc.).

#### ACKNOWLEDGEMENTS

The authors gratefully acknowledge the financial support from FONDECYT, project Nr. 1141158. A.M.R. thanks CONICYT-Chile for a doctoral scholarship folio 21130607.

#### References

1. J. M. Margolis, *Conductive Polymers and Plastics*, Chapman and Hall, New York (1989).
2. T. A. Skotheim, *Handbook of Conducting Polymers*, Marcel Dekker, New York (1998).
3. J. L. Reddinger and J. R. Reynolds, *Molecular engineering of pi-conjugated polymers. Radical Polymerisation of Polyelectrolytes*, v. 145 (1999).
4. M. Shahinpoor, *Electrochim. Acta*, 48 (2003) 2343.
5. J. W. Schultze and H. Karabulut, *Electrochim. Acta*, 50 (2005) 1739.
6. L. Zhang, Y. P. Wen, Y. Yao, J. K. Xu, X. M. Duan and G. Zhang, *Electrochim. Acta*, 116 (2014) 343.
7. G. Heywang and F. Jonas, *Adv. Mater.*, 4 (1992) 116.
8. M. Dietrich, J. Heinze, G. Heywang and F. Jonas, *J. Electroanal. Chem.*, 369 (1994) 87.
9. J. C. Gustafsson, B. Liedberg and O. Inganäs, *Sol. St. Ion.*, 69 (1994) 145.
10. G. A. Sotzing, J. R. Reynolds and P. J. Steel, *Chem. Mater.*, 8 (1996) 882.
11. J. C. Carlberg and O. Inganäs, *J. Electrochem. Soc.*, 144 (1997) L61.
12. L. Huchet, S. Akoudad, J. Roncali, *Adv. Mater.*, 10 (1998) 541.
13. M. C. Morvant and J. R. Reynolds, *Synth. Met.*, 92 (1998), 57.
14. A. Lima, P. Schottland, S. Sadki and C. Chevrot, *Synth. Met.*, 93 (1998) 33.
15. J. Heinze, B. A. Frontana-Urbe and S. Ludwigs, *Chem. Rev.*, 110 (2010) 4724.

16. S. Y. Abe, L. Ugalde, M. A. del Valle, Y. Tregouet and J. C. Bernede, *J. Braz. Chem. Soc.*, 18 (2007) 601.
17. R. Salgado, R. del Rio, M. A. del Valle and F. Armijo, *J. Electroanal. Chem.*, 704 (2013) 130.
18. R. Salgado, M. A. del Valle, B. G. Duran, M. A. Pardo and F. Armijo, *J. Appl. Electrochem.*, 44 (2014) 1289.
19. M. A. del Valle, P. Llanquileo, F. R. Diaz, M. Faundez, L. A. Hernandez and B. Gonzalez, *J. Chil. Chem. Soc.*, 59 (2014) 2481.
20. P. Liu, H. X. Yang, X. P. Ai, G. R. Li and X. P. Gao, *Electrochem. Commun.*, 16 (2012) 69.
21. A. G. MacDiarmid, *Synth. Met.*, 125 (2001) 11.
22. M. A. del Valle, M. Gacitua, F. R. Diaz, F. Armijo and J. P. Soto, *Electrochim. Acta*, 71 (2012) 277.
23. R. Schrebler, M. A. del Valle, H. Gomez, C. Veas and R. Cordova, *J. Electroanal. Chem.*, 380 (1995) 219.
24. G. C. Arteaga, M. Antilen, M. Faundez, F. R. Diaz, F. Armijo, L. A. Hernandez, A. Ramos and M. A. del Valle, *Int. J. Electrochem. Sci.*, 8 (2013) 2898.
25. G. C. Arteaga, M. A. del Valle, M. Antilen, M. Faundez, M. A. Gacitua, F. R. Diaz, J. C. Bernede and L. Cattin, *Int. J. Electrochem. Sci.*, 6 (2011) 5209.
26. M. A. del Valle, G. M. Soto, L. Guerra, J. H. Velez and F. R. Diaz, *Polym. Bull.*, 51 (2004) 301.
27. M. I. S. Depinto, H. T. Mishima and B. A. L. Demishima, *J. Appl. Electrochem.*, 27 (1997) 831.
28. R. Cordova, M. A. del Valle, A. Arratia, H. Gomez and R. Schrebler, *J. Electroanal. Chem.*, 377 (1994) 75.
29. R. Schrebler, P. Grez, P. Cury, C. Veas, M. Merino, H. Gomez, R. Cordova and M. A. del Valle, *J. Electroanal. Chem.*, 430 (1997) 77.
30. M. A. del Valle, P. Cury and R. Schrebler, *Electrochim. Acta*, 48 (2002) 397.
31. M. A. del Valle, L. Ugalde, F. del Pino, F. R. Diaz and J. C. Bernede, *J. Braz. Chem. Soc.*, 15 (2004) 272.
32. M. A. del Valle, M. A. Gacitua, L. I. Canales and F. R. Diaz, *J. Chil. Chem. Soc.*, 54 (2009) 260.
33. G. C. Arteaga, M. A. del Valle, M. Antilen, M. Romero, A. Ramos, L. Hernandez, M. C. Arevalo, E. Pastor and G. Louarn, *Int. J. Electrochem. Sci.*, 8 (2013) 4120.
34. M. A. del Valle, M. Romero, F. R. Diaz, F. Armijo, R. del Rio, I. Nuñez and E. A. Dalchiele, *Int. J. Electrochem. Sci.*, 8 (2013) 12321.
35. M. Romero, M. A. del Valle, R. del Rio, F. R. Diaz, F. Armijo and E. A. Dalchiele, *J. Electrochem. Soc.*, 160 (9) (2013) G125.
36. G. A. East and M. A. del Valle, *J. Chem. Ed.*, 77 (2000) 97.
37. M. A. del Valle, M. B. Camarada, F. Diaz and G. East, *e-Polymers*, 8(1) (2008) 839.
38. Chemicalize.org was used for generating structure property prediction and calculations, Marvin 6.2.4, 2014, chemicalize.org (<http://www.chemicalize.org>).
39. A. R. Hillman, S. J. Daisley and S. Bruckenstein, *Electrochim. Acta*, 53 (2008) 3763.
40. C. Kvarnstrom, H. Neugebauer, S. Blomquist, H. J. Ahonen, J. Kankare and A. Ivaska, *Electrochim. Acta*, 44 (1999) 2739.
41. A. R. Hillman, S. J. Daisley and S. Bruckenstein, *Phys. Chem. Chem. Phys.*, 9 (2007) 2379.
42. H. Randriamahazaka, V. Noel and C. Chevrot, *J. Electroanal. Chem.*, 476 (1999) 183.
43. E. Tamburri, S. Orlanducci, F. Toschi, M. L. Terranova and D. Passeri, *Synth. Met.*, 159 (2009) 406.
44. A. J. Downard and D. Pletcher, *J. Electroanal. Chem.*, 206 (1986) 139.